



Double trouble? Quantifying the risk from co-exposure to multiple pathogens in *Tenebrio molitor* at different CO₂ concentrations

Pascal Herren^{a,b,c}, Claus Svendsen^a, Carlotta Savio^{d,e}, Nicolai V. Meyling^b, Alison M. Dunn^c, Helen Hesketh^{a,*}

^a UK Centre for Ecology & Hydrology, Maclean Building, Benson Lane, Crowmarsh Gifford, Wallingford, Oxfordshire OX10 8BB, United Kingdom

^b Department of Plant and Environmental Sciences, University of Copenhagen, Thorvaldsensvej 40, 1871 Frederiksberg, Denmark

^c Faculty of Biological Sciences, University of Leeds, Leeds LS2 9JT, United Kingdom

^d INRAE, AgroParisTech, Micalis Institute, Université Paris-Saclay, Domaine de Vilvert, 78350 Jouy-en-Josas, France

^e Laboratory of Entomology, Wageningen University, Department of Plant Sciences, 6708 PB Wageningen, the Netherlands

ARTICLE INFO

Keywords:

Co-infection

Antagonism

Bacillus thuringiensis

Metarhizium brunneum

Carbon dioxide

Mass-reared insects

ABSTRACT

The insect mass-rearing industry to produce feed and food is expanding rapidly. Insects in production frequently encounter multiple pathogens and environmental stressors simultaneously, which can lead to significant economic losses. Our understanding of the interactions between different stressors remains limited, and existing methods primarily focus on determining overall patterns of additivity, synergism, or antagonism. However, the interactions between different stressors may exhibit more intricate response patterns, such as time or dose dependency. With the expanding industry of insect production, it becomes vital to conduct comprehensive risk assessment of diseases, using approaches that can detect both lethal and sublethal effects. Here, we assessed the risk of co-exposure to a fungal (*Metarhizium brunneum*) and a bacterial (*Bacillus thuringiensis*) pathogen in the yellow mealworm (*Tenebrio molitor*) at ambient and elevated carbon dioxide (CO₂) concentrations. We assessed total larval biomass per treatment group, survival, and individual weight gain 14 and 20 days after pathogen exposure. To analyse the data, we used a mixture toxicity (MIXTox) model, which identifies dose ratio or dose level dependency in addition to overall antagonism or synergism. The interactions between the two pathogens were mostly antagonistic or additive at both CO₂ concentrations and time points, indicating that the observed effects during co-exposure did not exceed the expected combined effects of the individual exposure. We did not find evidence that the interactions between the pathogens substantially change at elevated CO₂. The antagonistic interactions measured in the bioassays are likely to be indirect via the insect host, as we did not detect direct inhibition between the two pathogens in *in vitro* experiments. Here we show that using the MIXTox model is a powerful tool to assess the effects of co-exposure to pathogens and quantify risk of disease in mass-reared insects.

1. Introduction

The production of insects as feed and food is an alternative to traditional sources of protein such as livestock, soy, or fishmeal (Hawkey et al., 2021). This new industry is rapidly expanding and is predicted to reach an annual production of 500,000 tons of insect protein by 2030 (de Jong and Nikolik, 2021). Mass-reared insects are at an increased risk of infections by entomopathogens (insect pathogens) due to the high densities they are cultured in (Eilenberg et al., 2015; Maciel-Vergara et al., 2021), which can severely affect production (Eilenberg et al., 2015). Different pathogens may occur simultaneously in insect mass-

rearing systems (Maciel-Vergara et al., 2021). Furthermore, mass-reared insects may be exposed to environmental stress such as elevated temperature, humidity, or changes in gas concentrations (Herren et al., 2023; Maciel-Vergara et al., 2021). The interactions between stressors may be synergistic (i.e., larger effect than predicted), antagonistic (i.e., smaller effect than predicted), or additive (i.e., as predicted). For the risk assessment of the impact of individual stressors in insect mass-rearing systems, it is therefore critical to understand how they interact with other common stressors in the system.

Among the insect species reared for feed and food, the yellow mealworm, *Tenebrio molitor*, is considered one of the most promising

* Corresponding author.

E-mail address: hhesketh@ceh.ac.uk (H. Hesketh).

<https://doi.org/10.1016/j.jip.2025.108269>

Received 26 June 2024; Received in revised form 15 November 2024; Accepted 7 January 2025

Available online 9 January 2025

0022-2011/© 2025 The Author(s). Published by Elsevier Inc. This is an open access article under the CC BY license (<http://creativecommons.org/licenses/by/4.0/>).

species for industrial mass-rearing (Gkinali et al., 2022). *Tenebrio molitor* is susceptible to infection by various microbial entomopathogens (Slowik et al., 2023) with two important pathogens being the gram-positive bacterium *Bacillus thuringiensis* and the ascomycete fungus *Metarhizium brunneum* (Slowik et al., 2023). Both pathogens are a threat to the production of *T. molitor* as they can be introduced into the mass-rearing system via the feed (Bernhard et al., 1997; Wakil et al., 2014) and *B. thuringiensis* has recently been reported from a *T. molitor* rearing system (Leierer et al., 2023). In addition, mass-reared *T. molitor* may be exposed to elevated carbon dioxide (CO₂) concentrations in closed rearing systems (Kok, 2021). Concentrations of 5,000 ppm (parts per million) CO₂ have been reached in experimental setups with larval populations of *T. molitor* (Li et al., 2015), which is the set limit of legal long-term (8 h) human exposure in many countries (HSE, 2020; The US National Institute for Occupational Safety and Health, 2019). This CO₂ concentration, which is approximately 12 times higher than the ambient CO₂ concentration (415 ppm) (Keeling and Keeling, 2017), is therefore likely to occur in *T. molitor* mass-rearing systems. In a previous study, we showed that these industrially relevant CO₂ concentrations affect host-pathogen interactions in *T. molitor* larvae leading to higher survival rates of larvae exposed to *M. brunneum* or *B. thuringiensis* under elevated CO₂ concentrations (Herren et al., 2024). However, it remains unknown if, and how, the interactions change under co-exposure to the two tested pathogens.

Environmental conditions can have a direct effect on pathogens and insects outside of any host-pathogen interaction, but the environment can also affect pathogens indirectly via the host (e.g., via the insect's innate immune response) (Herren et al., 2023). Similarly, the interactions between co-infecting pathogens can either be direct (e.g., one pathogen produces a metabolite that inhibits or facilitates the other pathogen) or indirect (e.g., the host immune response is affected by one pathogen, resulting in an altered response to the other pathogen) (Staves and Knell, 2010). In the Colorado potato beetle (*Leptinotarsa decemlineata*) exposure to mixtures of *B. thuringiensis* and either of the entomopathogenic fungi *Beauveria bassiana*, *Metarhizium robertsii*, or *Metarhizium anisopliae* led to higher than expected mortality of the larvae (i.e., a synergistic interaction) (Kryukov et al., 2009; Wraight and Ramos, 2005; Yaroslavtseva et al., 2017) or no significant change in susceptibility (Costa et al., 2001). *Bacillus thuringiensis* inhibits feeding in infected hosts through disruption of gut membranes, which may in turn aid the fungal pathogen in the infection process of such weakened hosts (Furlong and Groden, 2003; Kryukov et al., 2009). In addition, *B. thuringiensis* infection inhibited the cellular immune response of *L. decemlineata* and it increased the germination of fungal conidia on the insect cuticle, which correlated with the synergistic interaction of higher observed mortality in co-infected larvae (Yaroslavtseva et al., 2017). In the larvae of the spotted asparagus beetle (*Crioceris quatuordecimpunctata*), a sublethal dose of *B. thuringiensis* toxin led to increased mortality when additionally exposed to *B. bassiana* (Gao et al., 2012). The authors showed that the larvae develop more slowly when exposed to the *B. thuringiensis* toxin, which increases the time between moults, possibly leading to increased penetration by *B. bassiana* (Gao et al., 2012). Moreover, *B. thuringiensis* in combination with destruxins (fungal secondary metabolites) of *M. anisopliae* led to synergistic or additive effects (i.e., increase or no change in mortality, respectively) in spruce budworm (*Choristoneura fumiferana*) larvae depending on the dose applied (Brousseau et al., 1998).

There are only few studies on the impact of co-infections in *T. molitor* and the simultaneous exposure to a bacterial and a fungal pathogen has, to our knowledge, not been tested to date. Moreover, there exists a gap in knowledge on how CO₂ affects host-pathogen interactions in mass-reared insects in general (Herren et al., 2023). The outcomes of co-exposure of insects to different stressors cannot be predicted without studying them together (i.e., simultaneously or sequentially) and interactions between entomopathogens are often investigated by using methods that only determine overall additivity, synergism, or

antagonism. However, interactions may follow more complex response patterns such as dose dependency (i.e., interactions change depending on the dose of the stressors applied) and time dependency (i.e., interactions change over time).

In this study, we tested if *M. brunneum* and *B. thuringiensis* interact in a synergistic way in *T. molitor* as has been shown for other insect species (Brousseau et al., 1998; Kryukov et al., 2009; Wraight and Ramos, 2005; Yaroslavtseva et al., 2017). In addition, we assess if the interactions between the two pathogens change under elevated CO₂ concentrations. Testing these different stressors in combination is crucial for the risk assessment of each stressor in *T. molitor* production systems for insect health. We use a mixture toxicity (MIXTox) model (Jonker et al., 2005) at different time points after exposure and *in vitro* assays to assess the interactions and thereby quantify the risks caused by co-exposures to different stressors. The MIXTox model was originally developed in the field of ecotoxicology to study interactions between chemicals. However, use of this model to study interactions between entomopathogens has been proposed by our laboratory (Hesketh et al., 2009). Using the MIXTox model has the advantage that dose-level dependent [i.e., “the deviation from either reference model at low dose levels is different from the deviation at high dose levels” (Jonker et al., 2005)] or dose-ratio dependent [i.e., “the deviation from either reference model depends on the composition of the mixture” (Jonker et al., 2005)] effects of mixtures can be detected (Jonker et al., 2005). Here, we demonstrate the use of the MIXTox model to study *in vivo* interactions between two entomopathogens.

2. Materials and methods

All experiments were conducted on two independent occasions (except for the initial establishment of EC₅₀ values, which was run once). The experiments were conducted in two 50-litre LEEC Culture Safe CO₂ incubators positioned adjacent to each other, set at 28 °C (±0.5 °C), 75 % (±5%) relative humidity, and ambient (450 ± 50 ppm) or elevated (4,500 ± 500 ppm) CO₂ concentrations, in complete darkness. The elevated CO₂ concentration was chosen based on our knowledge that CO₂ concentrations should never exceed 5,000 ppm in a working environment (Health and Safety Executive (HSE), 2020; The US National Institute for Occupational Safety and Health, 2019). Such levels are reached in *T. molitor* rearing systems (Li et al., 2015). Each of the incubators had 40 mm ELUTENG USB fans installed at the rear opening which were activated for 15 min at 45-minute intervals. The environmental conditions were monitored every 15 min using EasyLog EL-SIE-2 loggers for temperature and relative humidity and Rotronic CL11 loggers for CO₂ concentrations.

2.1. *Bacillus thuringiensis* culture

Bacillus thuringiensis serovar *morrisoni* biovar *tenebrionis* 4AA1 (*Bacillus* genetic stock center, Ohio State University, USA) was grown on LB-agar (lysogeny broth agar; 10 g tryptone, 5 g yeast extract, 10 g NaCl, and 15 g bacteriological agar in 1 l dH₂O) in plastic Petri dishes (9 cm diameter, triple vented) overnight at 30 °C. Subsequently, one bacterial colony was introduced into each of eight 500 ml Erlenmeyer flask that held 50 ml HCT medium (5 g tryptone, 2 g bacto casamino acids, 6.8 g KH₂PO₄, 0.1 g MgSO₄, 0.002 g MnSO₄, 0.014 g ZnSO₄, 0.15 g CaCl₂ and 0.022 Ammonium ferric citrate in 1 l dH₂O). The flasks were sealed with Parafilm™ and incubated for 96 h on a platform shaker (200 rpm at 30 °C). Afterwards, the suspension was centrifuged at 3,900 rpm (3,231 g, Eppendorf Centrifuge 5810 R) at 4 °C for 10 min. The resulting supernatant was disposed of and 20 ml of sterile dH₂O was added and the pellet re-suspended. After repeating this washing process twice using the aforementioned settings, the resulting stock suspension was incubated at 75 °C for 10 min. Confirmation of the presence of bacterial spores and crystals was performed by examining the suspension under a light microscope (Leica DM2000 LED; 1,000 times magnification). The number

6 × 10 ⁴ conidia/mg diet	<i>Mb</i>	<i>Mb</i> × <i>Bt</i>		
3 × 10 ⁴ conidia/mg diet	<i>Mb</i>	<i>Mb</i> × <i>Bt</i>	<i>Mb</i> × <i>Bt</i>	
10 ⁴ conidia/mg diet	<i>Mb</i>	<i>Mb</i> × <i>Bt</i>	<i>Mb</i> × <i>Bt</i>	<i>Mb</i> × <i>Bt</i>
Control	H ₂ O	<i>Bt</i>	<i>Bt</i>	<i>Bt</i>
	Control	2 × 10 ⁴ spores/mg diet	3 × 10 ⁵ spores/mg diet	5 × 10 ⁶ spores/mg diet

Fig. 1. Experimental design of the *in vivo* experiment conducted in the same way at ambient (450 ± 50 ppm) and elevated (4,500 ± 500 ppm) CO₂ concentrations. The treatments consisted of three individual *M. brunneum* (*Mb*) conidia concentrations, three individual *B. thuringiensis* (*Bt*) spore concentrations, six mixture treatments, and one control in both CO₂ concentrations. The preparation of the suspensions were prepared per ml, but they are given here as per mg diet. Two experimental repetitions were performed.

of colony forming units (cfu) per ml were assessed by plating 10 µl of ten-fold serial dilutions (10⁴–10⁹) of the stock suspension on LB-agar plates in triplicate and counting the number of cfu after 28 °C incubation for 16 h.

2.2. *Metarhizium brunneum* culture

Metarhizium brunneum isolate KVL12-30 (culture collection of the Department of Plant and Environmental Sciences, University of Copenhagen, Denmark) was cultured in plastic Petri dishes (9 cm diameter, triple vented) containing SDAY/4 medium (16.25 g Sabouraud dextrose agar, 2.5 g yeast extract, and 11.25 g agar in 1 l dH₂O) for 14 days at 28 °C in darkness. Thereafter, the conidia produced on the medium were suspended in TritonX-100 (0.05 % v/v) after agitating from the plate using a Drigalski spatula. The resultant suspension was centrifuged at 3,000 rpm (1,872 g, Eppendorf Centrifuge 5810 R) at 18 °C for 3 min before disposing of the supernatant and adding fresh TritonX-100 (0.05 % v/v). This washing procedure was repeated once using the aforementioned settings and afterwards sterile dH₂O was added to produce a stock suspension. The conidia concentration in the stock suspension was estimated by counting conidia in a 0.2 mm Fuchs-Rosenthal hemocytometer under a light microscope (400 times magnification). Fresh conidia suspensions were produced for each experiment on the day of use. Conidia germination was assessed alongside each experiment by spreading 100 µl of 10⁶ conidia/ml on Petri dishes (9 cm diameter, triple vented) containing SDAY/4 medium in triplicate and incubated for 18 h at 28 °C. Thereafter, 300 conidia per Petri dish were examined under a light microscope (400 times magnification) and germination was assessed; a conidium was counted as germinated if its germ tube was at least the length of the smallest diameter of the conidium.

2.3. Insect culture

Tenebrio molitor larvae were initially supplied by the company Ynsect (Evry, France) and reared in the laboratory for more than eight generations. For regular culturing, adult *T. molitor* (40 females and 40 males) were kept in 50 g diet (96 % w/w wheat bran and 4 % w/w dried egg white) and supplied with 5 g water agar (1 % w/v) in 750-ml containers (n = 6) for four days at ambient CO₂. Thereafter, the adults were removed and for the mixture experiment, the containers were distributed to incubators set at either ambient or elevated CO₂ concentrations. The initial assessment of EC₅₀ values was only done with larvae reared at ambient CO₂ concentrations (A. Supplementary methods). The larvae received 10 g water agar (1 % w/v) as a source of water twice a week, starting one week after removal of the adults.

2.4. *In vivo* mixture experiment

The larvae in each 750-ml container were distributed in groups of 30 larvae to empty 60-ml cups 17 days after removal of the adults. Larvae were subsequently starved for 24 h. Spore suspensions of *B. thuringiensis* (4 × 10⁷, 6 × 10⁸, and 10¹⁰ spores/ml) and conidia suspensions of *M. brunneum* (2 × 10⁷, 6 × 10⁷, and 1.2 × 10⁸ conidia/ml) were prepared as detailed previously. The concentrations for each pathogen in the medium was based on the EC₅₀ values (A. Supplementary methods) obtained for the endpoint of larval biomass (mg/cm²) 14 days after exposure (Table B1) to each pathogen separately. To prepare the individual pathogen suspensions, each of the aforementioned suspensions was mixed with dH₂O in a ratio 1:1. Mixture suspensions were prepared by mixing the aforementioned suspensions of *B. thuringiensis* spores and *M. brunneum* conidia in a ratio 1:1 (Fig. 1). Thereafter, 100 µl of the individual and mixture suspensions was added to 100 mg diet in 60-ml cups (n = 4 per treatment). The diet and suspension were mixed thoroughly with a sterile inoculation loop. Control cups were also prepared in the same way with 100 µl dH₂O in 100 mg diet (n = 5). Afterwards, 30 larvae were added to each of these cups containing the suspensions and the diet. This experiment was conducted at either ambient or elevated CO₂ concentrations at the same time. This resulted in 12 cups for the individual exposure to *B. thuringiensis*, 12 cups for the individual exposure to *M. brunneum*, 24 cups for the mixture exposure to both pathogens, and five cups for the control at either ambient or elevated CO₂ concentrations.

After two days of exposure to the pathogens, the larvae were moved to new cups containing clean diet (0.6 × fresh weight of larvae; this amount ensures no starving of larvae between feeding time points) and water agar (1 % w/v; 0.6 × fresh weight of larvae). All larvae were retained in their respective treatments at either ambient or elevated CO₂ concentrations for the entire duration of the experiment. Larvae were weighed in groups every second day for a total of 20 days. The total larval mass of each group at each time point was divided by the number of live larvae in that group to obtain the average individual weight of larvae. The individual weight at day 0 of the experiment was subtracted from the individual weight at each time point to obtain the individual weight gain. Any dead larvae were removed, and fresh diet and water agar were added as detailed before.

2.5. Effect of *M. brunneum* on *in vitro* spore viability of *B. thuringiensis*

Seven mixture suspensions of *B. thuringiensis* spore/crystal (10³ spores/ml) and *M. brunneum* conidia were prepared. The *B. thuringiensis*: *M. brunneum* ratios were 1:0; 1:3; 1:1.5; 1:0.5; 1:0.1; 1:0.033; 1:0.002. These ratios were chosen based on the ratios used in the *in vivo* experiments. For each suspension, 10 µl was added to Petri dishes (9 cm diameter, a 2 cm wide plastic strip was placed between each lid and dish base to allow for air circulation) containing 10 ml LB-agar (n = 9). By tilting the Petri dishes, the suspensions formed straight lines across the agar. After 16 h of incubation at either ambient or elevated CO₂ concentrations, the cfu were counted and used to calculate cfu/ml.

2.6. Effect of *B. thuringiensis* on *in vitro* germ tube length of *M. brunneum*

Seven mixture suspensions of *M. brunneum* conidia (10⁶ conidia/ml) and *B. thuringiensis* spore/crystal were prepared. The *M. brunneum*: *B. thuringiensis* ratios were 1:0; 1:500; 1:30; 1:10; 1:2; 1:0.66; 1:0.33. These ratios were chosen based on the ratios used in the *in vivo* experiments. For each suspension, 100 µl was spread on Petri dishes (9 cm diameter, a 2 cm wide plastic strip was put between each lid and dish base to allow for air circulation, n = 3) containing 10 ml bacteriological agar (15 g in 1 l dH₂O). After 15 h of incubation at either ambient or elevated CO₂ concentrations, three cover slips (22 × 22 mm) were added on each Petri dish. Six pictures were taken for each Petri dish (two per cover slip, location randomly chosen) using a Flexacam C3 mounted on a

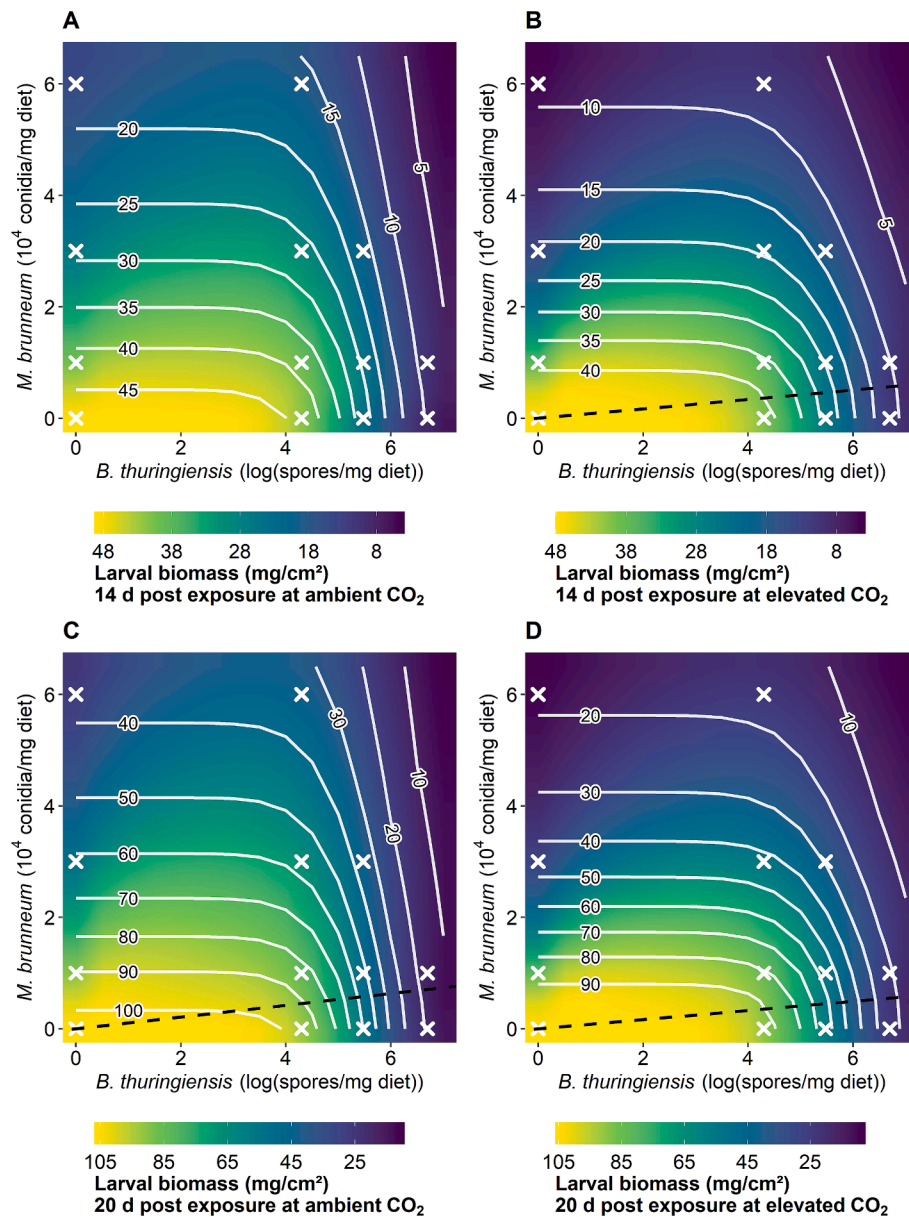


Fig. 2. Experimental repetition 1. Contour plots of the endpoint larval biomass (mg/cm²). The *B. thuringiensis* concentrations are plotted on the x-axes, the *M. brunneum* concentrations are plotted on the y-axes. The white isobole lines show independent action prediction of the joint effects, whereas the colour gradients show the outcome of the models that describe the data best (Table 2). The white crosses show the tested individual (along x- and y-axis) and mixture (inside the plots) concentrations. The black dotted lines mark the shifts from antagonism (above the dotted lines) to synergism (below the dotted lines) for data that was best described using the dose ratio-dependent deviation model. **A** 14 days post exposure to pathogens at ambient CO₂. **B** 14 days post exposure to pathogens at elevated CO₂. **C** 20 days post exposure to pathogens at ambient CO₂. **D** 20 days post exposure to pathogens at elevated CO₂.

light microscope (Leica DM2000 LED) at 1,000 times magnification. The lengths of all fungal germ tubes were measured using the segmented line tool in ImageJ 1.54d. Data from the ratio 1:500 was excluded from analysis because the fungal germ tubes could not be identified between the *B. thuringiensis* spores/crystal suspension.

2.7. Statistical analysis

2.7.1. The effect of CO₂ on individual pathogen concentration–response

The single pathogen concentration–response relationships of the mixture experiment were modelled by fitting the data to three-parameter log-logistic models using the ‘LL.3’ function in the ‘drc’ package (Ritz et al., 2015) using R v. 4.1.0 (R Core Team, 2021) given by the following equation:

$$y = \frac{\mu_{\max}}{1 + \left(\frac{c}{EC_{50}}\right)^\beta} \quad (1)$$

where *y* is the response (either larval biomass, survival, or weight gain) 14 days after exposure, μ_{\max} is the upper limit (i.e., response when the pathogen concentration is 0), *c* is the pathogen concentration, *EC*₅₀ is the pathogen concentration that results in 50 % reduction of μ_{\max} , and β is the slope parameter. The effect of exposure to different CO₂ concentrations was performed comparing *EC*₅₀ values using the ‘compParm’ function.

2.7.2. Mixture analysis

Data from the mixture experiment was analysed using the ‘MIXTox’ model (Jonker et al., 2005) assuming independent action as the

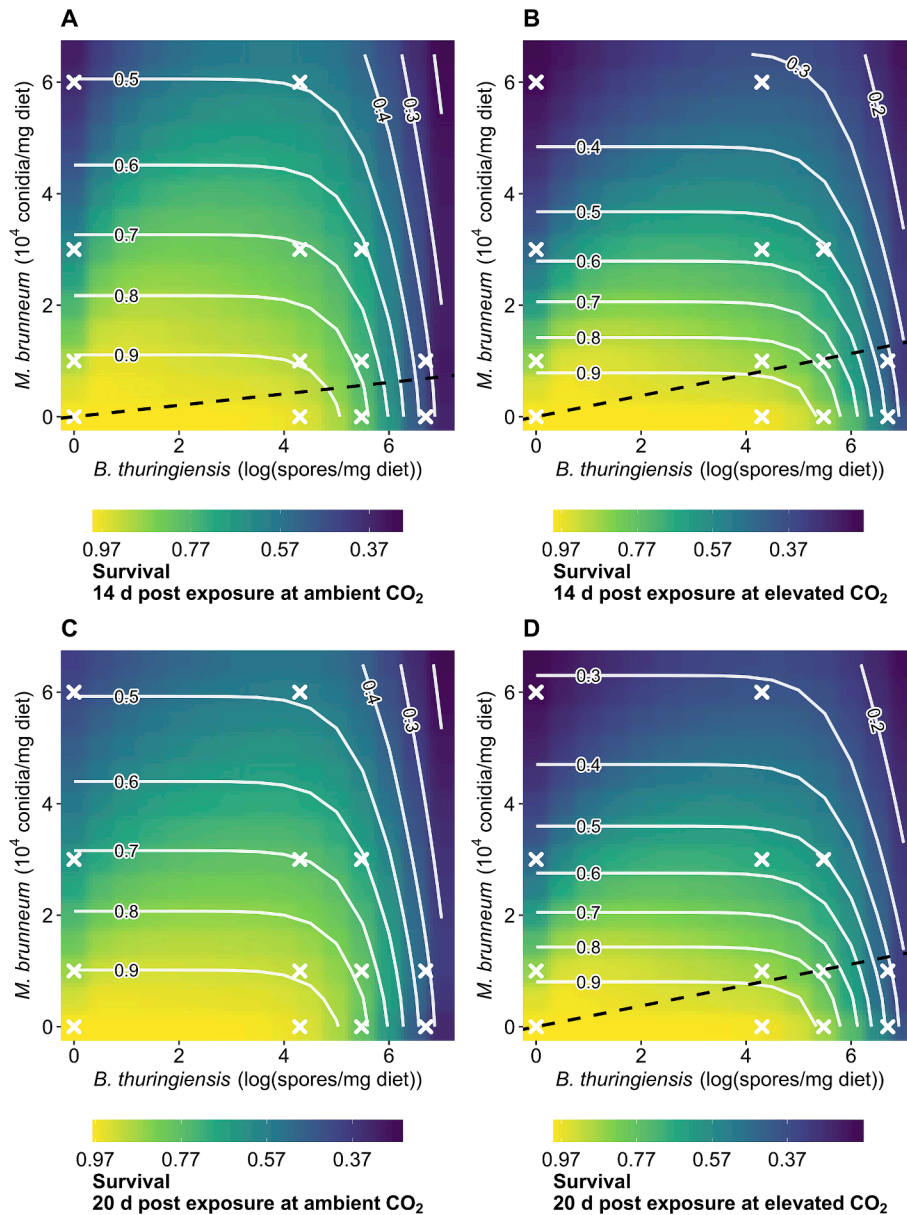


Fig. 3. Experimental repetition 1. Contour plots of the endpoint survival of larvae. The *B. thuringiensis* concentrations are plotted on the x-axes, the *M. brunneum* concentrations are plotted on the y-axes. The white isobole lines show independent action prediction of joint effects, whereas the colour gradients show the outcome of the models that describe the data best (Table 2). The white crosses show the tested individual (along x- and y-axis) and mixture (inside the plots) concentrations. The black dotted lines mark the shifts from antagonism (above the dotted lines) to synergism (below the dotted lines) for data that was best described using the dose ratio-dependent deviation model. **A** 14 days post exposure to pathogens at ambient CO₂. **B** 14 days post exposure to pathogens at elevated CO₂. **C** 20 days post exposure to pathogens at ambient CO₂. **D** 20 days post exposure to pathogens at elevated CO₂.

reference model for each endpoint given by the following equation:

$$y = \mu_{\max} \left(\frac{1}{1 + \left(\frac{c_{Mb}}{EC_{50Mb}} \right)^{\beta_{Mb}}} \right) \times \left(\frac{1}{1 + \left(\frac{c_{Bt}}{EC_{50Bt}} \right)^{\beta_{Bt}}} \right) \quad (2)$$

using the same parameters as noted above for *M. brunneum* (*Mb*) and *B. thuringiensis* (*Bt*) in equation (1). An F-test was performed to confirm that the reference model of independent action provided a statistically significant fit compared to the null hypothesis of no relationship between observed mixture effects and exposure concentrations. To check for significant interaction deviation patterns from the independent action model it was then extended by adding a parameter (*a*) to test if there was an overall synergistic or antagonistic interaction (Jonker et al., 2005). Thereafter, an additional parameter (*b*) was included to allow the

degree of synergism or antagonism to vary depending on the dose ratio in which the two stressors are present (parameter *b_{DR}*) or to allow the degree of synergism or antagonism to vary depending on the overall dose level of effect (parameter *b_{DL}*) (Jonker et al., 2005). The ‘Solver’ add-in function in Microsoft® Excel 2016 was used to fit the models to the data by minimising the sum of squared residuals. During all model fitting, care was taken to test a range of starting parameter values to ensure a global minimum was identified. The degree and significance of the improvement in fit achieved with the addition of the extra parameters was tested using Chi-square tests (*X*²) for all nested model pairs. To identify which of the nested models provided the best fit description of the observed dose–response surface, first independent action vs synergistic or antagonistic interaction (one d.f. different) were compared. Where the synergistic or antagonistic interaction model fitted significantly better, then the synergistic or antagonistic interaction model fit

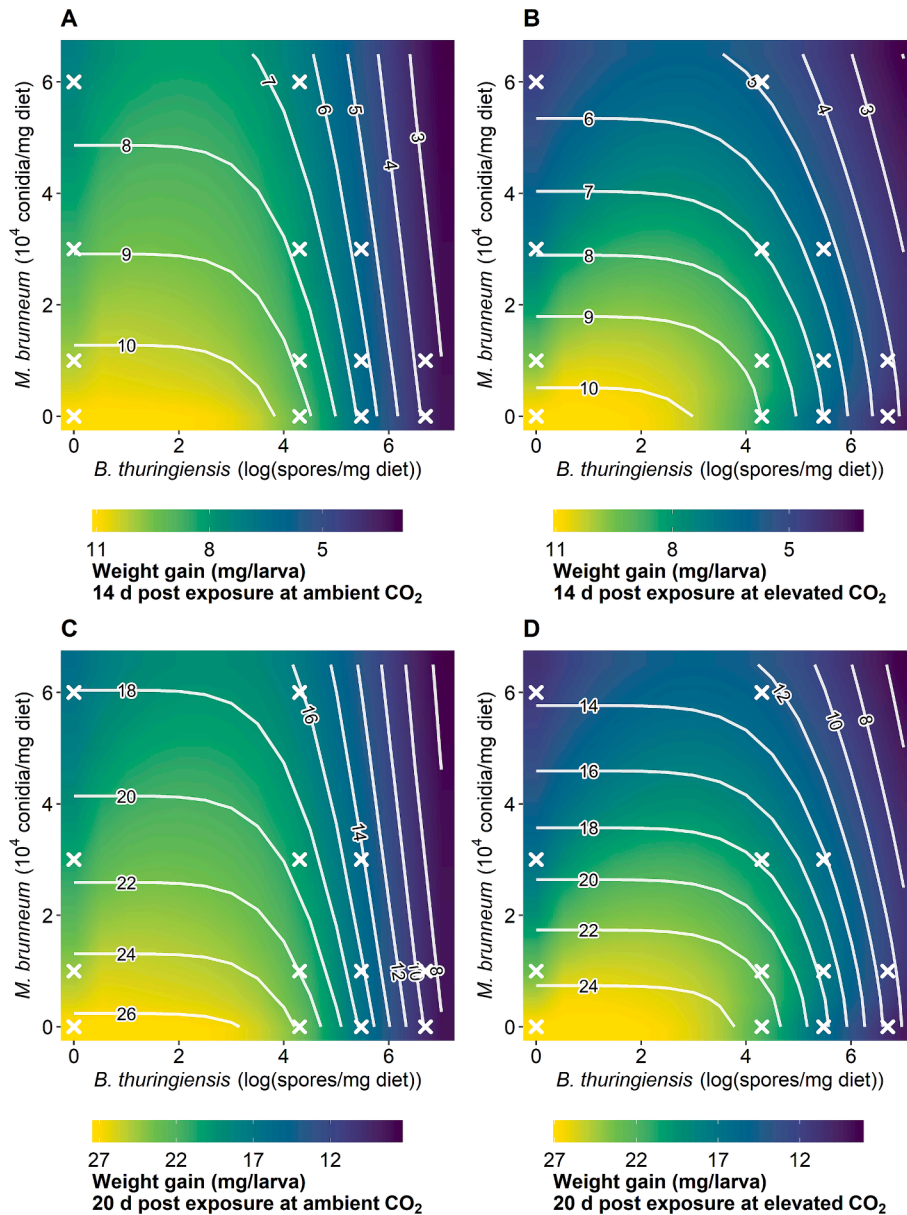


Fig. 4. Experimental repetition 1. Contour plots of the endpoint weight gain (mg/larva). The *B. thuringiensis* concentrations are plotted on the x-axes, the *M. brunneum* concentrations are plotted on the y-axes. The white isobole lines show independent action prediction of the joint effects, whereas the colour gradients show the outcome of the models that describe the data best (Table 2). The white crosses show the tested individual (along x- and y-axis) and mixture (inside the plots) concentrations. **A** 14 days post exposure to pathogens at ambient CO₂. **B** 14 days post exposure to pathogens at elevated CO₂. **C** 20 days post exposure to pathogens at ambient CO₂. **D** 20 days post exposure to pathogens at elevated CO₂.

was compared to the dose ratio-dependent deviation model and the dose level-dependent deviation model fits respectively (one d.f. different). Where the synergistic or antagonistic interaction model did not provide a significant improvement over the independent action model, any improvement of fit achieved by the dose ratio-dependent deviation model or the dose level-dependent deviation model was tested against the independent action model (two d.f. difference). Depending on the parameters of a , b_{DR} , and b_{DL} , different interaction patterns of antagonistic or synergistic effects are described as defined in Jonker et al. (2005). Where the dose ratio-dependent deviation model was identified as the best fit model, the switch ratio for the dose ratio-dependent deviation model were calculated using the following equation:

$$c_{Mb} = \left(\frac{-b_{DR}}{a} - 1 \right) \frac{ECx_{Mb}}{ECx_{Bt}} c_{Bt} \quad (3)$$

To understand how interactions may change temporally, we tested the interactions between *M. brunneum* and *B. thuringiensis* at both 14 and 20 days after exposure.

2.7.3. In vitro experiments

The data on germ tube length of *M. brunneum* and number of viable spores of *B. thuringiensis* were analysed using two-way analysis of variance (ANOVA) in R v. 4.1.0 (R Core Team, 2021). The two experimental repetitions were combined as there was no interactive effect of experimental repetition with treatment or CO₂ exposure found in initial three-way ANOVAs. The normality (QQ-plots) and homogeneity of variances (Levene test, $p > 0.05$) were tested to check if assumptions were satisfied. The data on germ tube length was log-transformed before analysis to satisfy assumptions. Tukey's HSD (Honestly Significant Difference) tests were used to separate means.

For all statistical analysis, differences were considered significant

Table 1
Experimental repetition 1. Results of MIXTOX models for larval biomass (Larv. biom. in mg/cm²), survival, and individual weight gain (Ind. weight gain in mg/larva) at ambient and elevated CO₂ either 14 or 20 days after pathogen exposure. Models that described the data best are highlighted in bold. IA, independent action; S/A, synergistic/antagonistic; DR, dose ratio-dependent; DL, dose level-dependent.

	14 days								20 days							
	Ambient CO ₂				Elevated CO ₂				Ambient CO ₂				Elevated CO ₂			
	IA	S/A	DR	DL	IA	S/A	DR	DL	IA	S/A	DR	DL	IA	S/A	DR	DL
Larv. biom.																
μ_{\max}	47.32	49.28	49.11	49.56	44.82	47.69	48.05	47.60	103.62	107.09	106.71	107.69	99.07	105.09	105.92	104.87
β_{Bt}	8.56	7.50	7.20	7.69	8.07	6.87	6.16	6.40	9.18	8.24	7.84	8.68	8.84	7.68	6.85	7.01
β_{Mb}	1.42	1.30	1.52	1.33	1.82	1.56	1.93	1.41	1.40	1.31	1.56	1.38	1.91	1.64	2.03	1.44
^a EC50 _{Bt}	5.68	5.41	5.49	5.40	5.88	5.49	5.57	5.49	5.67	5.43	5.51	5.42	5.88	5.51	5.59	5.52
^b EC50 _{Mb}	4.16	3.23	3.13	3.13	2.81	2.08	1.93	2.07	3.94	3.10	3.01	3.01	2.74	2.01	1.86	1.99
<i>a</i>	NA	1.63	3.74	1.07	NA	1.98	5.51	4.23	NA	1.57	3.99	0.45	NA	2.10	5.84	4.88
<i>b</i>	NA	NA	-4.09	-0.88	NA	NA	-6.84	0.76	NA	NA	-4.76	-4.04	NA	NA	-7.28	0.81
Residuals	1504.78	1178.07	1102.12	1176.14	1499.38	1077.15	915.00	1040.86	8274.43	6787.17	6310.01	6723.82	8261.33	5976.44	5173.39	5715.22
R ²	0.84	0.88	0.88	0.88	0.85	0.89	0.91	0.90	0.83	0.86	0.87	0.86	0.84	0.89	0.90	0.89
^c p(χ^2)	<0.001	<0.001	0.060	0.768	<0.001	<0.001	0.003	0.178	<0.001	0.001	0.049	0.481	<0.001	<0.001	0.006	0.124
Survival																
μ_{\max}	0.97	0.97	0.98	0.97	0.98	0.98	0.98	0.98	0.96	0.97	0.98	0.97	0.98	0.98	0.98	0.98
β_{Bt}	9.50	8.76	8.48	8.46	10.84	10.57	9.96	9.80	9.56	8.74	8.32	8.43	10.83	10.59	9.98	9.82
β_{Mb}	1.43	1.34	1.58	1.24	1.50	1.41	1.84	1.09	1.43	1.32	1.53	1.22	1.55	1.46	1.86	1.13
^a EC50 _{Bt}	6.59	6.44	6.54	6.45	6.65	6.54	6.70	6.56	6.60	6.44	6.53	6.42	6.65	6.55	6.69	6.56
^b EC50 _{Mb}	6.18	4.79	4.28	4.87	3.67	3.00	2.71	2.71	6.11	4.71	4.18	4.18	3.59	2.97	2.69	2.69
<i>a</i>	NA	1.88	4.84	2.87	NA	1.49	5.67	4.70	NA	1.87	4.67	3.43	NA	1.43	5.45	4.64
<i>b</i>	NA	NA	-5.60	0.71	NA	NA	-8.32	1.11	NA	NA	-5.26	0.69	NA	NA	-7.98	1.13
Residuals	100.68	77.26	72.42	76.87	89.35	71.56	56.66	69.72	98.72	75.96	73.97	77.21	85.74	69.50	55.97	67.33
R ²	0.75	0.81	0.82	0.81	0.83	0.87	0.89	0.87	0.75	0.81	0.81	0.80	0.84	0.87	0.90	0.88
^c p(χ^2)	<0.001	<0.001	0.028	0.532	<0.001	<0.001	<0.001	0.175	<0.001	<0.001	0.159	NA	<0.001	<0.001	<0.001	0.141
Ind. weight gain																
μ_{\max}	10.84	11.10	11.21	11.22	10.20	11.05	11.01	11.15	26.49	27.42	27.17	27.36	24.93	27.06	26.89	27.28
β_{Bt}	5.60	4.96	4.85	5.09	5.20	3.85	3.82	3.47	6.11	5.22	5.27	5.50	6.08	4.33	4.28	3.91
β_{Mb}	1.08	0.89	1.06	1.06	1.52	1.21	1.26	1.06	0.99	0.95	1.02	0.98	1.48	1.17	1.27	1.01
^a EC50 _{Bt}	6.00	5.86	5.81	5.78	6.36	5.79	5.84	5.76	6.13	5.93	6.02	5.92	6.52	5.99	6.07	5.98
^b EC50 _{Mb}	12.74	12.74	9.45	9.45	6.76	4.70	4.70	4.70	12.92	9.48	9.48	9.48	6.81	4.51	4.51	4.51
<i>a</i>	NA	1.12	1.86	0.12	NA	2.15	2.60	5.38	NA	1.35	3.02	0.02	NA	2.37	3.20	5.68
<i>b</i>	NA	NA	-0.95	-19.03	NA	NA	-0.86	0.93	NA	NA	-2.78	-121.13	NA	NA	-1.64	0.93
Residuals	50.23	45.67	44.48	44.19	89.61	66.68	66.51	64.63	335.58	292.79	287.64	287.44	605.53	437.14	433.44	423.46
R ²	0.83	0.85	0.85	0.85	0.68	0.76	0.76	0.77	0.81	0.83	0.83	0.83	0.64	0.74	0.75	0.75
^c p(χ^2)	<0.001	0.025	0.237	0.186	<0.001	<0.001	0.714	0.198	<0.001	0.007	0.332	0.323	<0.001	<0.001	0.502	0.194

^a in log(spores/mg diet).

^b $\times 10^4$ conidia/mg diet.

^c resulting from F-test for IA (IA vs Null model), or from Chi-square tests (χ^2) for S/A (IA vs S/A), DR (DR vs S/A), and DL (DL vs S/A).

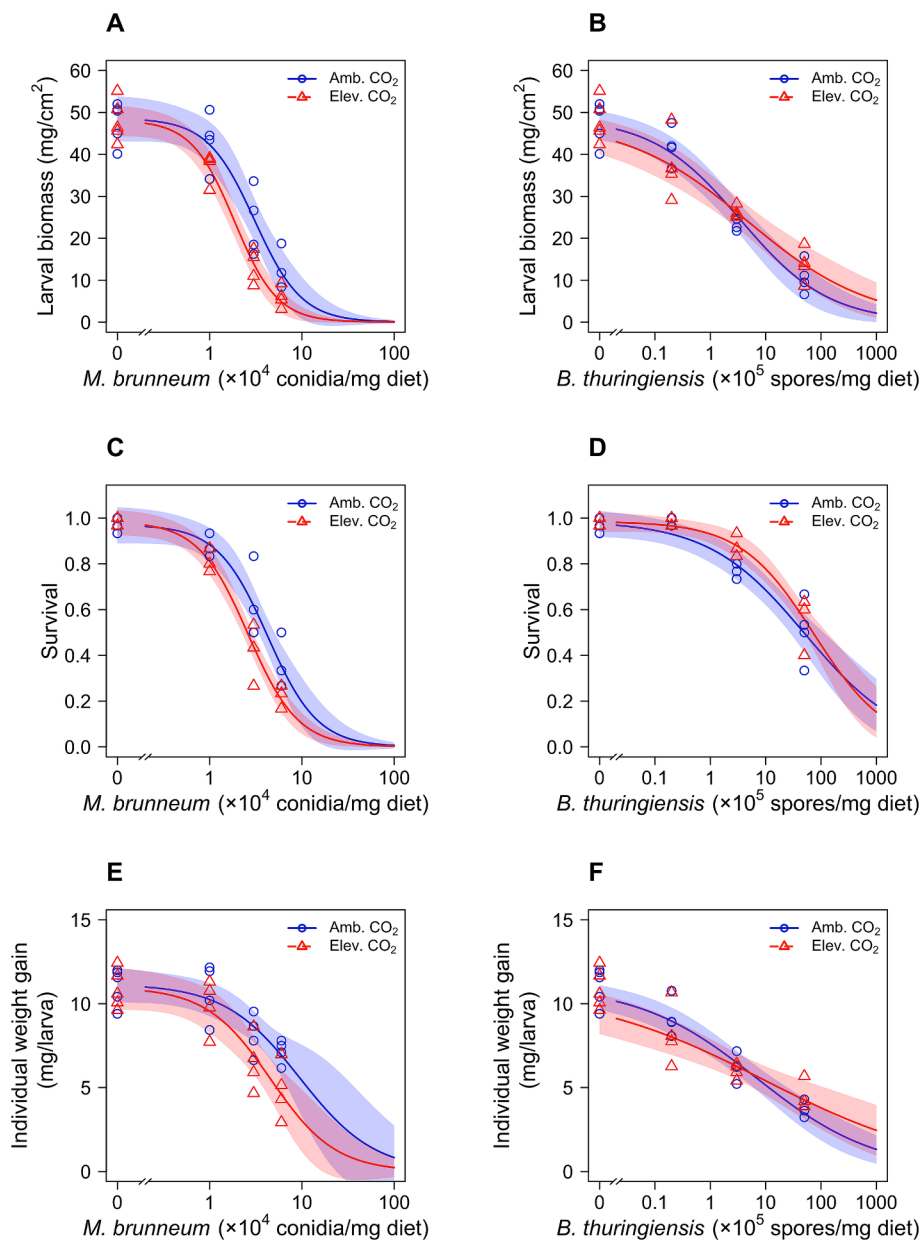


Fig. 5. Experimental repetition 1. Three-parameter log-logistic models of larval biomass, survival, and individual weight gain of larvae exposed to individual pathogen concentrations at either ambient (Amb.; blue, circles) or elevated (Elev.; red, triangles) CO₂ concentrations 14 days after exposure. **A** Larval biomass (mg/cm²) after *M. brunneum* exposure. **B** Larval biomass (mg/cm²) after *B. thuringiensis* exposure. **C** Survival after *M. brunneum* exposure. **D** Survival after *B. thuringiensis* exposure. **E** Individual weight gain (mg/larva) after *M. brunneum* exposure. **F** Individual weight gain (mg/larva) after *B. thuringiensis* exposure. (For interpretation of the references to colour in this figure legend, the reader is referred to the web version of this article.)

when the p -value was < 0.05 .

3. Results

3.1. Mixture analysis

The results of the mixture toxicity analyses for larval biomass, survival, and individual weight gain for the experimental repetition 1 are visualised in Figs. 2, 3, and 4, respectively. An antagonistic interaction in this study was found when survival, total larval biomass, or individual weight gain were higher than predicted from the independent action reference model, whereas a synergistic interaction was found when these endpoints were lower than predicted from the independent action reference model. The conidial viability of *M. brunneum* conidia was $\geq 99\%$ in all experiments.

In the experimental repetition 1, the parameter a was > 0 in all cases, which indicates antagonism between the two pathogens. Adding parameter a by using the synergistic or antagonistic interaction models for larval biomass, survival, and weight gain of larvae (Table 1) significantly decreased the residuals at both time points and CO₂ concentrations, and provided a significantly improved fit (as indicated by the Chi-square tests values [$p(\chi^2)$] all being below 0.05). The subsequent addition to some of the data sets of the additional parameter b further improved the fit to the data. Adding parameter b using dose ratio-dependent deviation further decreased the residuals for larval biomass at ambient CO₂, 20 days post exposure and at elevated CO₂, 14 and 20 days post exposure. Survival was also better described by the dose ratio-dependent deviation model than the synergistic or antagonistic interaction model at ambient CO₂, 14 days post exposure and at elevated CO₂, 14 and 20 days post exposure. For all endpoints that were better

Table 2

Experimental repetition 1. EC₅₀ values, slopes (β) and upper limits (μ_{\max}) of three-parameter log-logistic models of larval biomass (mg/cm²), survival, and individual weight gain (mg/larva) of larvae exposed to individual pathogen (*M. brunneum* or *B. thuringiensis*) concentrations at either ambient (Amb.) or elevated (Elev.) CO₂ concentrations 14 days after exposure. EC₅₀ values followed by different letters for the same endpoint and pathogen indicate significant differences among the treatments. SE, standard error.

	Larval biomass (mg/cm ²)		Survival		Individual weight gain (mg/larva)	
	Amb. CO ₂	Elev. CO ₂	Amb. CO ₂	Elev. CO ₂	Amb. CO ₂	Elev. CO ₂
<i>M. brunneum</i>						
^a EC ₅₀ ± SE	3.07 ± 0.43a	1.86 ± 0.17b	4.24 ± 0.45a	2.61 ± 0.20b	9.45 ± 2.99a	4.60 ± 0.90a
β ± SE	1.70 ± 0.38	1.86 ± 0.24	1.60 ± 0.32	1.60 ± 0.17	1.07 ± 0.38	1.24 ± 0.36
μ_{\max} ± SE	48.61 ± 2.60	48.17 ± 1.73	0.97 ± 0.04	0.98 ± 0.03	11.17 ± 0.53	10.98 ± 0.64
<i>B. thuringiensis</i>						
^b EC ₅₀ ± SE	3.52 ± 1.09a	1.86 ± 0.17a	51.26 ± 17.20a	74.93 ± 15.35a	6.99 ± 2.54a	9.43 ± 6.25a
β ± SE	0.54 ± 0.08	1.86 ± 0.24	0.50 ± 0.09	0.66 ± 0.12	0.40 ± 0.06	0.27 ± 0.06
μ_{\max} ± SE	48.78 ± 1.88	48.17 ± 1.73	0.99 ± 0.03	0.99 ± 0.02	11.10 ± 0.41	10.90 ± 0.51

^a × 10⁴ conidia/mg diet.

^b × 10⁵ spores/mg diet.

described using the the dose ratio-dependent deviation model model, parameter *a* was > 0 and parameter *b* was < 0 indicating antagonism when the mixture was dominated by *M. brunneum* switching to synergism when the mixture was dominated by *B. thuringiensis*. The shifts between antagonism (above dotted lines) and synergism (below dotted lines) are shown in Figs. 2 and 3 (only applicable for figures in which dose ratio-dependent deviations were used).

The results of the mixture toxicity analyses for larval biomass, survival, and individual weight gain for the experimental repetition 2 are visualised in Figs. B.2, B.3, and B.4, respectively. As shown in Table B2 the experimental repetition 2, adding parameter *a* to the independent action model for larval biomass 20 days post exposure at ambient CO₂ significantly decreased the residuals. Similarly, residuals were significantly decreased by adding parameter *a* to the independent action models for survival 14 and 20 days post exposure at ambient CO₂. Similar to the experimental repetition 1, parameter *a* was > 0 indicating antagonism. Moreover, residuals were significantly reduced when using the dose ratio-dependent deviation model to describe individual weight gain 14 days after pathogen exposure at elevated CO₂ with *a* > 0 and *b* < 0. All the data from other endpoints in the experimental repetition 2 were best described using independent action.

3.2. The effect of CO₂ on individual pathogen concentration-responses

We compared the responses of *T. molitor* (larval biomass, survival, and individual weight gain) when exposed to the two individual pathogens at the two CO₂ concentrations (Fig. 5, Fig. B5). The comparison of the EC₅₀ values revealed that for larval biomass and survival the EC₅₀ values were lower for larvae exposed to *M. brunneum* under elevated CO₂ in the experimental repetition 1, i.e., the larvae were more susceptible to the fungus under these conditions (Table 2). However, there were no differences between the EC₅₀ values of larvae exposed to *M. brunneum* reared under different CO₂ concentrations in the experimental repetition 2 (Table B3). Moreover, there were no differences between EC₅₀ values for larvae exposed to *B. thuringiensis* under the different CO₂ concentrations in either of the two experimental repetitions (Table 2, Table B3). The *p* and *t* values of the comparisons between the EC₅₀ values are shown in Table B4.

Table 3

Results of two-way ANOVAs when *M. brunneum* (*Mb*) conidia were added to a fixed concentration of *B. thuringiensis* (*Bt*) spores (first row) and when *Bt* spores were added to a fixed concentration of *Mb* (second row).

	Mixture			CO ₂			Mixture × CO ₂		
	<i>F</i>	<i>P</i>	d.f.	<i>F</i>	<i>p</i>	d.f.	<i>F</i>	<i>p</i>	d.f.
<i>Mb</i> added to <i>Bt</i> : viability of <i>Bt</i> spores (cfu/ml)	1.43	0.205	6	16.96	<0.001	1	1.07	0.383	6
<i>Bt</i> added to <i>Mb</i> : <i>Mb</i> germ tube length (µm)	7.72	<0.001	5	608.61	<0.001	1	1.46	0.201	5

3.3. In vitro experiments

When different concentrations of *M. brunneum* conidia were applied in the *in vitro* experiments there was no effect on the viability of *B. thuringiensis* spores. However, elevated CO₂ decreased the viability of *B. thuringiensis* spores significantly (Table 3, Table B5). The addition of different concentrations of *B. thuringiensis* spores to *M. brunneum* had a significant effect on their germ tube length with a trend of increasing germ tube lengths with increasing *B. thuringiensis* spore concentrations at elevated CO₂ (Table 3). The subsequent Tukey HSD test, however, did not reveal any significant differences between pathogen mixture treatments (Table B6). Furthermore, the germ tubes of *M. brunneum* were significantly longer at elevated CO₂ (Table B6).

4. Discussion

Our results show that in this series of experiments, the majority of the interactions between the bacterium *B. thuringiensis* and the ascomycete fungus *M. brunneum* were modelled as either antagonistic or additive at ambient and elevated CO₂ concentrations. This indicates that the risk of infection in the larval stage does generally not increase by exposure to a mixture of the two pathogens at the tested CO₂ concentrations. Synergism between *M. brunneum* and *B. thuringiensis* in terms of effects on *T. molitor* larvae only occurs when the mixture is dominated by *B. thuringiensis*. However, most of the modelled areas on the figures that were described as synergism within the model were outside the tested mixture treatments. Even though we have found synergistic interactions only in very specific cases, several previous studies have reported synergistic interactions between *B. thuringiensis* and other fungal pathogens in other insect species (Kryukov et al., 2009; Wraight and Ramos, 2005; Yaroslavtseva et al., 2017). Wraight and Ramos (2005) tested mixtures that were dominated by *B. thuringiensis* (Wraight and Ramos, 2005) and their finding of synergistic interactions is in accordance with our results, as we also only found synergism when the mixtures were dominated by *B. thuringiensis*. Kryukov et al. (2009) and Yaroslavtseva et al. (2017), in contrast, reported synergistic interactions for mixtures in which the fungal pathogen (i.e., *M. anisopliae*, *B. bassiana*, or *M. robertsii*) was dominating. However, the level of synergism was variable in the different experiments conducted in these studies and only three out of

nine mixtures resulted in > 10 % mortality compared to the independent action reference model [data extracted from figures in Kryukov et al. (2009) and Yaroslavtseva et al. (2017) using (PlotDigitizer, 2023)].

Several authors suggested that the delayed development or starvation of insects exposed to *B. thuringiensis* could be responsible for synergistic interactions during mixed exposure with a fungal pathogen (Gao et al., 2012; Wraight and Ramos, 2005), with smaller larvae generally being more susceptible to pathogens (e.g., Hesketh-Best et al., 2021; Hesketh and Hails, 2015). However, even though exposure to *B. thuringiensis* significantly reduced larval biomass and individual weight gain in our experiments, the interactions with *M. brunneum* were mostly antagonistic or additive. The fact that we found antagonistic interactions between pathogens but no evidence of direct inhibition between the pathogens in the *in vitro* experiments, suggests that there is an indirect interaction via the insect host.

In the insect immune system, the Toll pathway is induced in response to fungal pathogens and gram-positive bacteria (Vogel et al., 2022). Medina Gomez et al. (2018) suggested that the Toll pathway in response to *B. thuringiensis* and *M. anisopliae* is highly expressed in *T. molitor* larvae. Exposure to the faster-acting *B. thuringiensis* therefore might have induced the Toll pathway, which could lead to better protection in larvae to the infection of *M. brunneum*, a hypothesis that remains to be tested. Antagonism has been reported in a system in which chickpea (*Cicer arietinum*) plants were inoculated with *B. bassiana* as an endophyte and combined with *B. thuringiensis*. In these experiments, the mixture of pathogens were reported as leading to synergistic, antagonistic, or additive interactions in larvae of the lepidopteran cotton bollworm (*Helicoverpa armigera*), depending on the dose of *B. thuringiensis* applied (Wakil et al., 2020). However, when the expected mortalities in these experiments are calculated using independent action (in the same way as we did in our analysis), we can only detect additive and synergistic interactions but no antagonistic interaction.

Our results on the effect of CO₂ concentrations on larvae exposed to *M. brunneum* on survival and larval biomass are variable, with differing results from the two experimental repetitions of the bioassay. In a previous study we conducted with single concentrations of the two pathogens we found increased survival of larvae exposed to elevated CO₂ (Herren et al., 2024). Despite the same CO₂ concentrations being tested in both the current and previous study, the data are not directly comparable because different pathogen concentrations were applied. The *in vivo* interactions between the two pathogens were relatively stable at the two time points (14 and 20 days after exposure). At ambient CO₂ there were slight changes between the two time points from overall antagonism at 14 days to dose-ratio dependency with major antagonism at 20 days for larval biomass and vice-versa for survival in the experimental repetition 1. In the experimental repetition 2, there was one change from independent action to overall antagonism for larval biomass. Furthermore, there was a change from the dose ratio-dependent deviation model to independent action for individual weight gain at elevated CO₂ in the experimental repetition 2. Similarly, there was no general trend when comparing the *in vivo* interactions at the two CO₂ concentrations suggesting that the tested CO₂ concentrations only have little or no effect on the pathogen interactions.

We found a significant effect of the pathogen mixture treatment on *M. brunneum* conidia germ tube lengths showing a trend to increasing germ tube lengths with increasing *B. thuringiensis* concentration at elevated CO₂. However, any differences among treatments could not be identified after the post-hoc test. Similarly, a previous study found that more conidia of *M. robertsii* germinated on the cuticles of *L. decemlineata* larvae infected with *B. thuringiensis*, than on the cuticles of control larvae (Yaroslavtseva et al., 2017). This is, however, likely to be an indirect effect of *B. thuringiensis* mediated by the insect host because the two pathogens did not come into direct contact in this experiment (Yaroslavtseva et al., 2017). In another study no effect of *B. thuringiensis* on the development and growth of *M. anisopliae* or *B. bassiana* was found (Kryukov et al., 2009). Moreover, Kryukov et al. (2009) found that

M. anisopliae weakly inhibited *B. thuringiensis* growth but this effect waned after 15–20 h (Kryukov et al., 2009). In our experiment, we measured spore viability of *B. thuringiensis* 16 h after application on artificial media, which could explain why we did not find an inhibitory effect of *M. brunneum* on *B. thuringiensis* spore viability.

We found a significant increase of the conidial germ tube lengths of *M. brunneum* at elevated CO₂ concentration, which is in accordance with a previous study that showed faster germination of *M. brunneum* conidia at elevated CO₂ (Herren et al., 2024). Increased germination of conidia at elevated CO₂ has also been described for another entomopathogenic fungus (*Entomophaga maimaiga*) (Hajek et al., 2002). Furthermore, we found a tendency for lower spore viability of *B. thuringiensis* at elevated CO₂, which is comparable to a previous study (Herren et al., 2024).

The method we describe here to examine interactions between pathogens allows a thorough analysis of potential interactions, including those which may be dose-level or dose-ratio dependent (Jonker et al., 2005). Using the MIXTox model affords an opportunity to test interactions between different pathogen species in *T. molitor* or other economically important insect species. In addition, this model could also be used to understand interactions between different environmental stressors or between pathogens and environmental stressors. As the field of insect mass-production is moving forward rapidly, methods to quantify risks of different stressors on insect health are essential to protect reared insects and ensure optimised production. Although interactions for different endpoints can be quantified by using the MIXTox model, additional methods are needed to understand the mechanisms underlying the outcomes, such as the measurements we made of direct interactions between pathogens *in vitro*. Further studies could focus on the innate immune response, following mixed infections to shed light on the mechanism or mechanisms involved. Moreover, the interactions between entomopathogens may be time-dependent, and sequential occurrence of different pathogens might result in altered interactions compared to simultaneous occurrence (Souza et al., 2019).

Our findings demonstrate that interactions between the pathogens *M. brunneum* and *B. thuringiensis* can range from synergism to antagonism, most likely mediated through the host insect. Notably, most combinations do not significantly increase the risk of disease measured as survival, or total larval biomass or individual larval weight gain in *T. molitor*. The MIXTox model proves to be a powerful tool to investigate co-exposure to pathogens and quantify risks in mass-reared insects and identify high risk combination ratios where treating insect stocks remedially for effects of one of the pathogens would yield greater benefits than addressing the other. In addition, this tool may potentially benefit other fields of invertebrate pathology research, such as biological control of insect pests using microbial biopesticides, offering potential use in evaluating and optimising the efficacy of mixed pathogen applications.

CRediT authorship contribution statement

Pascal Herren: Writing – original draft, Visualization, Methodology, Investigation, Formal analysis, Data curation, Conceptualization. **Claus Svendsen:** Writing – review & editing, Resources, Methodology, Conceptualization. **Carlotta Savio:** Writing – review & editing, Methodology. **Nicolai V. Meyling:** Writing – review & editing, Supervision, Funding acquisition, Conceptualization. **Alison M. Dunn:** Writing – review & editing, Supervision, Funding acquisition, Conceptualization. **Helen Hesketh:** Writing – review & editing, Supervision, Resources, Funding acquisition, Conceptualization.

Funding

This work was done within the project ‘Insect Doctors’ which has received funding from the European Union’s Horizon 2020 research and innovation programme under the Marie Skłodowska-Curie grant agreement No. 859850.

Declaration of competing interest

The authors declare that they have no known competing financial interests or personal relationships that could have appeared to influence the work reported in this paper.

Acknowledgements

We would like to thank ÿnsect for providing the initial *T. molitor* population. Furthermore, we would like to thank Daisy Fairchild and the late Alan Bloomfield (who is much missed by his colleagues) for the technical assistance.

Appendix A. Supplementary data

Supplementary data to this article can be found online at <https://doi.org/10.1016/j.jip.2025.108269>.

References

- Bernhard, K., Jarrett, P., Meadows, M., Butt, J., Ellis, D.J., Roberts, G.M., et al., 1997. Natural isolates of *Bacillus thuringiensis*: Worldwide distribution, characterization, and activity against insect pests. *J. Invertebr. Pathol.* 70, 59–68. <https://doi.org/10.1006/jipa.1997.4669>.
- Brousseau, C., Charpentier, G., Belloncik, S., 1998. Effects of *Bacillus thuringiensis* and destruxins (*Metarhizium anisopliae* mycotoxins) combinations on spruce budworm (Lepidoptera: Tortricidae). *J. Invertebr. Pathol.* 72, 262–268. <https://doi.org/10.1006/jipa.1998.4780>.
- Costa, S.D., Barbercheck, M.E., Kennedy, G.G., 2001. Mortality of Colorado potato beetle (*Leptinotarsa decemlineata*) after sublethal stress with the CryIIIA δ -endotoxin of *Bacillus thuringiensis* and subsequent exposure to *Beauveria bassiana*. *J. Invertebr. Pathol.* 77, 173–179. <https://doi.org/10.1006/jipa.2001.5017>.
- de Jong, B., Nikolik, G., 2021. No longer crawling: Insect protein to come of age in the 2020s. https://insectfeed.nl/wp-content/uploads/2021/03/Rabobank_No-Longer-Crawling-Insect-Protein-to-Come-of-Age-in-the-2020s_Feb2021-1.pdf (accessed 11 December 2022).
- Eilenberg, J., Vlask, J.M., Nielsen-LeRoux, C., Cappellozza, S., Jensen, A.B., 2015. Diseases in insects produced for food and feed. *J. Insects Food Feed* 1, 87–102. <https://doi.org/10.3920/jiff2014.0022>.
- Furlong, M.J., Groden, E., 2003. Starvation induced stress and the susceptibility of the Colorado potato beetle, *Leptinotarsa decemlineata*, to infection by *Beauveria bassiana*. *J. Invertebr. Pathol.* 83, 127–138. [https://doi.org/10.1016/S0022-2011\(03\)00066-1](https://doi.org/10.1016/S0022-2011(03)00066-1).
- Gao, Y.L., Oppert, B., Lord, J.C., Liu, C.X., Lei, Z.R., 2012. *Bacillus thuringiensis* Cry3Aa toxin increases the susceptibility of *Crioceris quatuordecimpunctata* to *Beauveria bassiana* infection. *J. Invertebr. Pathol.* 109, 260–263. <https://doi.org/10.1016/j.jip.2011.12.003>.
- Gkinali, A.-A., Matsakidou, A., Vasileiou, E., Paraskevopoulou, A., 2022. Potentiality of *Tenebrio molitor* larva-based ingredients for the food industry: A review. *Trends Food Sci. Technol.* 119, 495–507. <https://doi.org/10.1016/j.tifs.2021.11.024>.
- Hajek, A.E., Davis, C.I., Eastburn, C.C., Vermeylen, F.M., 2002. Deposition and germination of conidia of the entomopathogen *Entomophaga maimaiga* infecting larvae of gypsy moth, *Lymantria dispar*. *J. Invertebr. Pathol.* 79, 37–43. [https://doi.org/10.1016/S0022-2011\(02\)00010-1](https://doi.org/10.1016/S0022-2011(02)00010-1).
- Hawkey, K.J., Lopez-Viso, C., Brameld, J.M., Parr, T., Salter, A.M., 2021. Insects: A potential source of protein and other nutrients for feed and food. *Annu. Rev. Anim. Biosci.* 9, 333–354. <https://doi.org/10.1146/annurev-animal-021419-083930>.
- Herren, P., Hesketh, H., Meyling, N.V., Dunn, A.M., 2023. Environment-host-parasite interactions in mass-reared insects. *Trends Parasitol.* 39, 588–602. <https://doi.org/10.1016/j.pt.2023.04.007>.
- Herren, P., Dunn, A.M., Meyling, N.V., Savio, C., Hesketh, H., 2024. Effect of CO₂ concentrations on entomopathogen fitness and insect-pathogen interactions. *Microb. Ecol.* 87, 1–11. <https://doi.org/10.1007/s00248-024-02347-6>.
- Hesketh, H., Hails, R.S., 2015. *Bacillus thuringiensis* impacts on primary and secondary baculovirus transmission dynamics in *Lepidoptera*. *J. Invertebr. Pathol.* 132, 171–181. <https://doi.org/10.1016/j.jip.2015.09.008>.
- Hesketh, H., Svendsen, C., Hails, R.S., 2009. Defining the response of *Mamestra brassicae* to mixed infections. 42nd Annual Meeting of the Society for Invertebrate Pathology. Hesketh-Best, P.J., Mouritzen, M.V., Shandley-Edwards, K., Billington, R.A., Upton, M., 2021. *Galleria mellonella* larvae exhibit a weight-dependent lethal median dose when infected with methicillin-resistant *Staphylococcus aureus*. *Pathog. Dis.* 79, 1–9. <https://doi.org/10.1093/femspd/ftab003>.
- Health and Safety Executive (HSE), 2020. EH40/2005 Workplace exposure limits. Norwich 1-61. <https://www.hse.gov.uk/pubns/priced/eh40.pdf>.
- Jonker, M.J., Svendsen, C., Bedaux, J.J.M., Bongers, M., Kammenga, J.E., 2005. Significance testing of synergistic/antagonistic, dose level-dependent, or dose ratio-dependent effects in mixture dose-response analysis. *Environ. Toxicol. Chem.* 24, 2701–2713. <https://doi.org/10.1897/04-431r.1>.
- Keeling, R.F., Keeling, C.D., 2017. Atmospheric monthly *in situ* CO₂ data - Mauna Loa observatory, Hawaii (Archive 2021-09-07). Scripps CO₂ Program Data. UC San Diego Library Digital Collections. Doi: 10.6075/J08W3BHW.
- Kok, R., 2021. Preliminary project design for insect production: Part 1 – overall mass and energy/heat balances. *J. Insects Food Feed* 7, 499–509. <https://doi.org/10.3920/jiff2020.0055>.
- Kryukov, V.Y., Khodyrev, V.P., Yaroslavtseva, O.N., Kamenova, A.S., Duisembekov, B.A., Glupov, V.V., 2009. Synergistic action of entomopathogenic hyphomycetes and the bacteria *Bacillus thuringiensis* ssp. *morrisoni* in the infection of Colorado potato beetle *Leptinotarsa decemlineata*. *Appl. Biochem. Microbiol.* 45, 571–576. <https://doi.org/10.1134/S000368380905010X>.
- Leierer, D., Olmstead, M., Oppert, B., 2023. Sequencing to identify pathogens in *Tenebrio molitor*: Implications in insects farmed for food and feed. *Front. Insect Sci.* 3, 1–7. <https://doi.org/10.3389/finsc.2023.1059046>.
- Li, L., Xie, B., Dong, C., Hu, D., Wang, M., Liu, G., Liu, H., 2015. Rearing *Tenebrio molitor* L. (Coleoptera: Tenebrionidae) in the “Lunar Palace 1” during a 105-day multi-crew closed integrative BLSS experiment. *Life Sci. Space Res.* 7, 9–14. <https://doi.org/10.1016/j.lssr.2015.08.002>.
- Maciel-Vergara, G., Jensen, A.B., Lecocq, A., Eilenberg, J., 2021. Diseases in edible insect rearing systems. *J. Insects Food Feed* 7, 621–638. <https://doi.org/10.3920/jiff2021.0024>.
- Medina Gomez, H., Adame Rivas, G., Hernández-Quintero, A., González Hernández, A., Torres Guzmán, J.C., Mendoza, H.L., Contreras-Garduño, J., 2018. The occurrence of immune priming can be species-specific in entomopathogens. *Microb. Pathog.* 118, 361–364. <https://doi.org/10.1016/j.micpath.2018.03.063>.
- PlotDigitizer, 2023 PlotDigitizer: Version 3.1.5. <https://plotdigitizer.com> (accessed 02 November 2023).
- R Core Team, 2021 R: A language and environment for statistical computing. <https://www.R-project.org/> (accessed 01 February 2022).
- Ritz, C., Baty, F., Streibig, J.C., Gerhard, D., 2015. Dose-response analysis using R. *PLoS One* 10, 1–13. <https://doi.org/10.1371/journal.pone.0146021>.
- Slowik, A., Herren, P., Bessette, E., Lim, F., Hernández-Pelegrín, L., Savio, C., 2023. Harmful and beneficial symbionts of *Tenebrio molitor* and their implications for disease management. *J. Insects Food Feed* 9, 1381–1396. <https://doi.org/10.3920/JIFF2022.0171>.
- Souza, M.L., Sanches, M.M., Souza, D.A.d., Faria, M., Espinel-Correia, C., Sihler, W., Lopes, R.B., 2019. Within-host interactions of *Metarhizium rileyi* strains and nucleopolyhedroviruses in *Spodoptera frugiperda* and *Anticarsia gemmatilis* (Lepidoptera: Noctuidae). *J. Invertebr. Pathol.* 162, 10–18. <https://doi.org/10.1016/j.jip.2019.01.006>.
- Staves, P.A., Knell, R.J., 2010. Virulence and competitiveness: testing the relationship during inter- and intraspecific mixed infections. *Evolution* 64, 2643–2652. <https://doi.org/10.1111/j.1558-5646.2010.00999.x>.
- The US National Institute for Occupational Safety and Health, 2019 Carbon dioxide. (accessed 27 January 2022).
- Vogel, M., Shah, P.N., Voulgari-Kokota, A., Maistrou, S., Aartsma, Y., Beukeboom, L.W., et al., 2022. Health of the black soldier fly and house fly under mass-rearing conditions: Innate immunity and the role of the microbiome. *J. Insects Food Feed* 8, 857–878. <https://doi.org/10.3920/jiff2021.0151>.
- Wakil, W., Usman Ghazanfar, M., Yasin, M., 2014. Naturally occurring entomopathogenic fungi infecting stored grain insect species in Punjab, Pakistan. *J. Insect Sci.* 14, 1–7. <https://doi.org/10.1093/jisesa/ieu044>.
- Wakil, W., Tahir, M., Al-Sadi, A.M., Shapiro-Ilan, D., 2020. Interactions between two invertebrate pathogens: An endophytic fungus and an externally applied bacterium. *Front. Microbiol.* 11, 1–13. <https://doi.org/10.3389/fmicb.2020.522368>.
- Wraight, S.P., Ramos, M.E., 2005. Synergistic interaction between *Beauveria bassiana* and *Bacillus thuringiensis tenebrionis* based biopesticides applied against field populations of Colorado potato beetle larvae. *J. Invertebr. Pathol.* 90, 139–150. <https://doi.org/10.1016/j.jip.2005.09.005>.
- Yaroslavtseva, O.N., Dubovskiy, I.M., Khodyrev, V.P., Duisembekov, B.A., Kryukov, V.Y., Glupov, V.V., 2017. Immunological mechanisms of synergy between fungus *Metarhizium robertsii* and bacteria *Bacillus thuringiensis* ssp. *morrisoni* on Colorado potato beetle larvae. *J. Insect Physiol.* 96, 14–20. <https://doi.org/10.1016/j.jinsphys.2016.10.004>.